A COMPUTER-AIDED DETECTION AND DIAGNOSIS FOR MICROCALCIFICATIONS IN DIGITAL MAMMOGRAMS

Song Lixin, Gao jie, Zhang kaiyu, Shi Shengjun

Harbin university of science and technology
Harbin 150080, P. R. China
T.86-451-86396216; F. 86-451-86396201; E.lixins99@yahoo.com.cn.

Abstract

To the question that the microcalcifications (MCCs) in the mammography are extremely small, various shapes, different size, variable distributions, and low contrast. The intensity difference between suspicious areas and their surrounding tissues can be quite slim. According to the principle that microcalcificatins are relatively high-frequency components buried in the background of low-frequency components and very high-frequency noise in the mammograms, the paper presents a method to detection the microcalcifications by morphology and wavelet transform. And according to the principle that artificial neural network can implement classification through training, the paper presents a method to identificate the types of pathological changes by probability neural network (PNN). Experiments indicate that the algorithm not only has simple operation, and achieves high true positive detection rate(TPR) at the cost of low false positive(FP).

1. Introduction

Breast cancer is the second cause of death among women cancers. There is one person die of breast cancer each 13 minutes. There is clear evidence which shows that early diagnosis and treatment of breast cancer can significantly increase the chance of survival for patients. Since the cause of breast cancer is still unknown, the earlier the cancer is detected, the better the chance that a proper treatment can be prescribed.

Detection methods are based on clinical examination, mammography, ultrasound, and core biopsy. Of these methods, mammography is the only reliable and practical method capable of detecting breast cancer at its early stage. Between 30%~50% of all breast malignancy exhibit microcalcifications, and the key technology of early diagnosis of breast cancer is to find the MCC in the mammography and estimate the tendency of malign. MCCs normally have a higher X-ray attenuation than the normal breast tissue and appear as a group of small localized granular bright structures in the mammograms. Two typical mammograms with MCC clusters are shown in Figure 1(a), (b) and the ROIs include suspicious MCC are shown in Figure 1(c), (d).

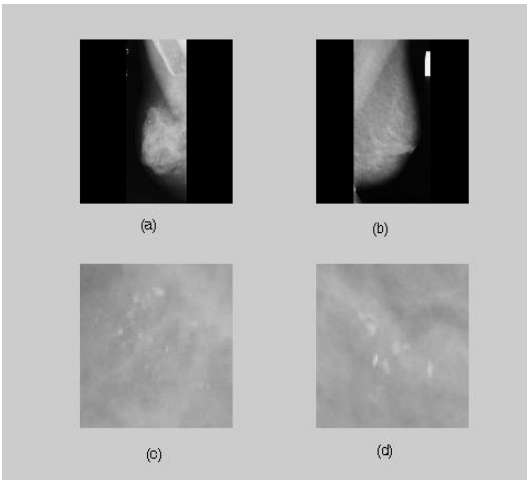

Figure 1. (a), (b) Typical mammograms with MCCs. (c), (d) ROIs which include MCCs

At present, the main methods of detecting MCCs include tradition image processing technology, wavelet transform, morphology, an artificial neural network etc. and the combining of several methods[1][2][3][4][5]. The single method above has higher TPR, but at the same time has higher FP.

This paper presents a computer-aided detection for clustered MCCs and classification the region of interest (ROI) into benign or malignant. The method proposed first extracts the suspicious MCC area (ROI) from the image using the (x, y) coordinates and radius value already provided by radiologist in the database MIAS. Our method has two separate steps. In the first step, we use morphological approach to isolate the breast background from the MCCs and gain a bilevel image I_m (x,y), and use wavelet transform to detection the MCCs and also gain a bilevel image I_w (x, y), then make a logical and operation I_m (x, y) and I_w (x, y) to realize the detection of MCCs. In the second step, an artificial neural network PNN is used to estimate the likelihood of malignancy or benign using the extracted features as input.

2. Microcalcification Detection

MCCs appear as tiny, circular deposits of calcium, which can vary in size from 0.1mm~1mm and usually marginally brighter than the background. From an image processing point of view, MCCs are relatively high-frequency components buried in the background of low-frequency components and very high-frequency noise in the mammograms. So, in the first step, the aim is to delete the low-frequency and very high-frequency components and realize the detection of MCCs. We use the top-hat transform of morphological approach to separate the MCCs from the background and use the wavelet transform to delete a part of the low-frequency and very high-frequency signal, and then utilize the logical and operation to gain the location of MCCs.

2.1. Morphological

MCCs appear on the mammography as circular bright spots, and a calcification has approximately a size of 20 pixels on each mammogram[2], so we chose a structuring element larger than 20 pixels. And they have low contrast. The properties of MCCs enable them to be detected through morphological approach.

Let $f(x, y)$ be an image and g be a structuring element. Then the elementary operation Erosion and Dilation are defined as follows (1-D):

$$f \Theta g = \wedge\{f_{-x} - g(x) : x \in D[g]\} \quad (1)$$

$$f \oplus g = \vee\{f_x + g(x) : x \in D[g]\} \quad (2)$$

Where $\wedge$ and $\vee$ are defined as follows:

$$(f \wedge g)(x) = \min\{f(x), g(x)\} \quad (3)$$

$$(f \vee g)(x) = \max\{f(x), g(x)\} \quad (4)$$

By combining erosion and dilation, the important morphological filter operations opening and closing are formed:

$$f \circ g = (f \Theta g) \oplus g \quad (5)$$

$$f \bullet g = -[(-f) \circ (-g)] \quad (6)$$

A gray value image is imagined to be a 2-D surface in 3-D space. An opening operation to the ROI keep the breast background and this means the positive peaks in the gray-value surface smaller than the structuring element are removed, and the structuring element chose is a little larger than the maximal size of MCC. Therefore the impossible MCCs are removed by opening operation. So we subtract this background from the original image to recover the positive peaks:

$$HAT(f) = f - (f \circ g) \quad (7)$$

Then we threshold the result image $HAT(f)$ using the value of 3.4σ, σ is the standard deviation of the result image.

Figure 2 shows the processing result using morphological.

2.2. Wavelet Transform

Since wavelets are localized in both the space and frequency domains, they have a multiresolution property. This makes it suitable for extracting MCCs from low-frequency backgrounds and high-frequency noise [6]. In particular, the wavelet transform decomposes the signal into signal bands of different frequency ranges. It can help to identify useful information relevant to MCCs and discard the signal bands which make little contribution to detection.

(a) (b) (c)

Figure 2. The ROI and the detection result using morphological. (a) ROI. (b) The image after Top-Hat operation. (c) The image after global thresholding

The wavelet used in this study is Daubechies orthogonal wavelet of length four. The ROIs are decomposed up to four levels using the wavelet transform. The 2-D scaling and wavelet function are defined as follow:

$$\phi(x,y) = \phi(x)\phi(y) \quad (8)$$

$$\psi^1(x,y) = \psi(x)\psi(y) \quad (9)$$

$$\psi^2(x,y) = \psi(x)\phi(y) \quad (10)$$

$$\psi^3(x,y) = \phi(x)\psi(y) \quad (11)$$

Where $\phi(x)$ and $\psi(x)$ are 1-D wavelet and scaling function.

Let $f(x,y)$ be an gray image, and it can be decomposed by the wavelet transform as follows:

$$A_j(m,n) = < f(x,y), \phi_{j,m,n}(x,y) > \quad (12)$$

$$D_j^1(m,n) = < f(x,y), \psi_{j,m,n}^1(x,y) > \quad (13)$$

$$D_j^2(m,n) = < f(x,y), \psi_{j,m,n}^2(x,y) > \quad (14)$$

$$D_j^3(m,n) = < f(x,y), \psi_{j,m,n}^3(x,y) > \quad (15)$$

Here, A is low frequency components; D^1, D^2, D^3 are horizontal, vertical and diagonal high-frequency components.

We generalized the wavelet decomposition by multiplying certain weighting value at each level *j* to enhance MCCs as well as suppressing background structures and noise. The reconstruction image $f'(x,y)$ is given by:

$$f'(x,y) = \alpha A_L(m,n) + \beta \sum_{j=2}^{L} (D_j^1(m,n) + D_j^2(m,n) + D_j^3(m,n)) + \chi(D_1^1(m,n) + D_1^2(m,n) + D_1^3(m,n)) \quad (16)$$

The wavelet used in this study is Daubechies orthogonal wavelet of length four. The ROIs are decomposed up to four levels using the wavelet transform. We chose to do the reconstruction by weakening LL_4 (corresponding the low-frequency background) and HL_1, LH_1, HH_1 (corresponding the very high-frequency noise) and enhancing $HL_{2,3}$, $LH_{2,3}$, $HH_{2,3}$. The reconstruction image is shown in Figure 3(a). And then using global threshold gain the location of MCCs. The bilevel image is shown in Figure 3(b).

2.3. Logic AND operation

In order to realize the detection of MCCs, we use logical AND operation to utilize the advantage of morphological approach and wavelet transform

$$I_r(x, y) = I_m(x, y) \text{ AND } I_w(x, y) \quad (17)$$

Eventually we realize the detection of MCCs. The result of logical AND operation is shown in Figure 3(c).

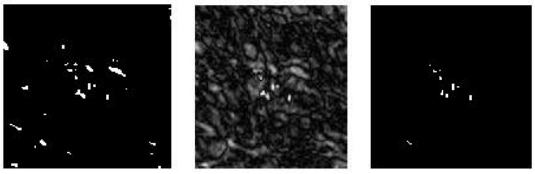

(a) (b) (c)

Figure 3. Detection result using wavelet and logical AND. (a) The reconstruction image $I_{w0}(x, y)$. (b) The bilevel image after global threshold $I_w(x,y)$. (c) The location of MCCs $I_r(x,y)$

3. Classify ROIs into Malignant or Benign

We extract features from the ROI and the bilevel image $I_r(x,y)$ separately, then utilize PNN to classify the ROIs into malignant or benign. The feature set is consisted of eight features. They are the pixel intensity variance (var), the energy variance (evar), the average (avg), the average-energy (eavg), the skewness (skew), and the kurtosis (kurt) from the original ROI, and the number of MCCs (num), the Euler number (eul) from the bilevel image.

We have selected PNN for classification purpose, which has 2 layers. When an input is presented, the first layer computes distances from the input vector to the training input vectors, and produces a vector whose elements indicate how close the input is to a training input. The second layer sums these contributions for each class of inputs to produce as its net output a vector of probabilities. Finally, a compete transfer function on the output of the second layer picks the maximum of these probabilities, and produces a 1 for that class and a 0 for the other classes.

Our method was evaluated with 50 ROI images (64×64 pixels) including 14 benign ROIs, 15 malignant ROIs and 21 ROI without MCCs. We use 35 ROIs being randomly selected for the training, and the rest 15 ROIs for testing.

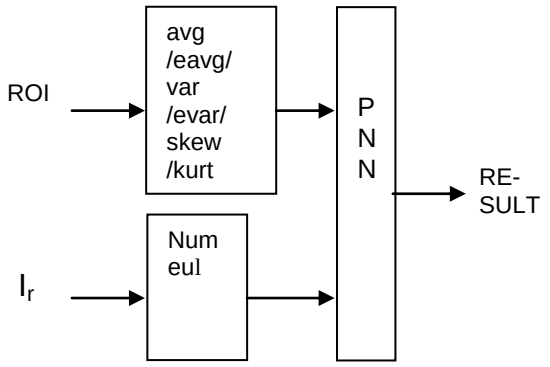

Figure 4. Mixed feature neual neural network for classifying the ROIs

4. Results and Discussions

The result of the detection of MCCs is shown in the Table 1. It achieves a 80.2% mean true positive detection rate at the cost of 2.45 false positive per ROI.

Table 1. The Results of Detection

ROI	The number of MCCs	Results	
		TPR	FP
Total	294	236/294(80.2%)	2.45

We utilize the PNN to classify the ROIs into malignant, benign and without MCCs. The recognition accuracy is 83.3% considering the malignant ROIs alone, 75% for the benign ROIs, and 60% for the ROIs without MCCs alone. The total accuracy is 73.3%. The results are expressed in terms of True Positive (TP). The results are shown in Table 2.

Table 2. Recognition score

	No. of ROIs	TPR	
		Training set	Test set
Malignant	15	8/9(88.9%)	5/6(83.3%)
Benign	14	10/10(100%)	3/4(75%)
without MCCs	21	14/16(93.8%)	3/5(60%)
Total	50	32/35(91.4%)	11/15(73.3%)

5. Conclusion

In this paper, we use wavelet transform and morphology to automatically detect MCCs in digitized mammograms. Use PNN Classify ROIs into Malignant or Benign. The proposed method is very efficient for automatically detect and Classify MCCs in mammograms. The conclusions are as follows: the combining of wavelet transform and morphology ensure higher TPR and reducing the FP.

References

[1] Noha Youssry, Fatma E.Z. Abou-Chadi and Alaa' M.El-Sayad. "Early detection of masses in digitized mammograms using texture features and neuro-fuzzy model", Proc. Of 4th International IEEE EMBS Special Topic Conference on Information Technology Applications in Biomedicine, 2003, pp. 226–229.

[2] Wan Mimi Diyana, Julie Larcher, and Rosli Besar. "A comparison of clustered microcalcifications automated detections in digital mammogram", Proc. Of ICASSP'03, 2, 2003, pp. 385-388.

[3] Wang T.C, Karayiannis N.B. "Detection of microcalcifications in digital mammograms using wavelets", IEEE Trans. Med. Imaging, 17(4), 1998, pp.498–509.

[4] H.D.Cheng, and Jingli Wang. "Fuzzy Logic and Scale Space Approach to Microcalcification Detection", Proc. Of ICASSP'03, 2, 2003, pp.345-348.

[5] Michael Wirth, Matteo Fraschini, Jennifer Lyon. "Contrast enhancement of microcalcifications in mammograms using morphological enhancement and non-flat structuring elements", Proceedings of the 17th IEEE Symposium on CBMS'04, 2004, pp.1063-7125.

[6] Songyang Yu, and Ling Guan. "A CAD System for the Automatic Detection of Clustered Microcalcifications in Digitized Mammogram Films", IEEE Trans. Med. Imag.,19(1), 2000, pp. 115-126.